



Bioinformatic gene analysis for possible biomarkers and therapeutic targets of hypertension-related renal cell carcinoma

Wenjie Huang^{1#}, Ke Wu^{1#}, Ruoyu Wu¹, Zhiguo Chen¹, Wei Zhai², Junhua Zheng¹

¹Department of Urology, Shanghai General Hospital, Shanghai Jiao Tong University School of Medicine, Shanghai, China; ²Department of Urology, Renji Hospital, School of Medicine in Shanghai Jiao Tong University, Shanghai, China

Contributions: (I) Conception and design: J Zheng, W Zhai; (II) Administrative support: J Zheng; (III) Provision of study materials or patients: W Huang, K Wu; (IV) Collection and assembly of data: R Wu, Z Chen; (V) Data analysis and interpretation: W Huang, K Wu; (VI) Manuscript writing: All authors; (VII) Final approval of manuscript: All authors.

[#]These authors contributed equally to this work.

Correspondence to: Junhua Zheng, Shanghai General Hospital, Shanghai 200080, China. Email: zhengjh0471@sina.com.cn; Wei Zhai, Department of Urology, Renji Hospital, Shanghai 200127, China. Email: jacky_zw2002@hotmail.com.

Background: Renal cell carcinoma (RCC) is one of the most prevalent malignant tumors of the urinary system. Hypertension can cause hypertensive nephropathy (HN). Meanwhile, Hypertension is considered to be related to kidney cancer. We analyzed co-expressed genes to find out the relationship between hypertension and RCC and show possible biomarkers and novel therapeutic targets of hypertension-related RCC.

Methods: We identified the differentially expressed genes (DEGs) of HN and RCC through analyzing Gene Expression Omnibus (GEO) datasets GSE99339, GSE99325, GSE53757 and GSE15641 by means of bioinformatics analysis, respectively. Then we evaluated these genes with protein-protein interaction (PPI) networks, Gene Ontology (GO) analysis, Kyoto Encyclopedia of Genes and Genomes (KEGG) pathway analysis and CTD database. Subsequently, we verified co-expressed DEGs with Gene Expression Profiling Interactive Analysis (GEPIA) database. Finally, corresponding predicted miRNAs of co-expressed DEGs were identified and verified via mirDIP database and Starbase, respectively.

Results: We identified 9 co-expressed DEGs, including *BCAT1*, *CORO1A*, *CRIP1*, *ESRRG*, *FN1*, *LYZ*, *PYCARD*, *SAP30*, and *PTRF*. *CRIP1* and *ESRRG* and their corresponding predicted miRNAs, especially hsa-miR-221-5p, hsa-miR-205-5p, hsa-miR-152-3p and hsa-miR-137 may be notably related to hypertension-related RCC.

Conclusions: *CRIP1* and *ESRRG* genes have great potential to become novel biomarkers and therapeutic targets concerning hypertension-related RCC.

Keywords: Biomarkers; computational biology; hypertension; renal cell carcinoma (RCC)

Submitted Mar 25, 2020. Accepted for publication Sep 25, 2020.

doi: 10.21037/tau-20-817

View this article at: <http://dx.doi.org/10.21037/tau-20-817>

Introduction

Renal cell carcinoma (RCC) is a common subtype of malignant tumor in the urinary system. Its incidence rate was 11.281 per 100,000 person-years. The incidence of RCC in men is higher than that in women (1). Around the world, the incidence of RCC is higher in developed countries than in developing countries (2). According to

cancer statistics 2020, in 2020 about 73,750 (4.1%) newly diagnosed kidney cancer cases are expected and around 14,830 (2.4%) will die of this cancer (3). In China, the incidence of RCC is the second highest in malignant tumors of the urinary system. Its incidence and mortality vary greatly from region to region and are higher in cities than in rural areas (4). Clear cell renal cell carcinoma

(ccRCC) is the most important type in RCC. According to the statistics, it accounts for around 80–90% of RCC (5). Although the early detection of RCC has been improved in recent years, more than one third of patients have local advanced tumor or metastatic disease at the time of diagnosis (6). The treatment remains a challenge and reliable biomarkers are essential to prevent metastasis and improve the quality of patients' life (7). Although some possible biomarkers have been found such as Ki-67, p53, VEGF, there is currently no reliable biomarker for RCC prediction (8). RCCs are usually resistant to conventional chemotherapy and almost all chemotherapeutic agents are ineffective against metastatic RCC (9). The use of targeted therapy is contributed to surgery in patients with locally advanced or metastatic RCC. Although some therapeutic targets have been applied, such as VEGFR and HIF-1 α , our exploration of therapeutic targets is far from enough (7).

Hypertension is a widespread chronic disease with an increased incidence worldwide (10). Hypertension is an important risk factor for kidney cancer (11). Hypertensive nephropathy (HN) is one of the main complications of hypertension. Over the past few years, the relationship between hypertension and the risk of kidney cancer have been explored by many prospective studies (12–14). In the VITAL study, hypertension was independently associated with RCC risk (HR 1.70; 95% CI, 1.30–2.22) (15). A meta-analysis of prospective studies shows a strong positive correlation between hypertension and kidney cancer. A history of hypertension was associated with 67% increased risk of RCC. Considering heterogeneity and publication bias, each 10 mmHg increase in blood pressure was associated with 10–22% increased risk of RCC (16). However, the molecular mechanism of the relationship between kidney cancer and hypertension is not clear. For these reasons, the identification of key molecular involved in hypertension-related kidney cancer is urgent and highly demanded to improve the clinical outcome. In our research, HN-related DEGs (HN-DEGs) and RCC-related DEGs (RCC-DEGs) were identified by bioinformatic analysis. Then co-expressed DEGs (co-DEGs) of HN and RCC were found. Furthermore, further analysis and verification of DEGs and predicted targeted miRNAs were conducted for HN patients inclined to RCC to find possible molecular mechanisms. We present the following article in accordance with the MDAR reporting checklist (available at <http://dx.doi.org/10.21037/tau-20-817>).

Methods

Gene expression profiles data

We downloaded GSE99339, GSE99325, GSE53757 and GSE15641 datasets from GEO (<http://www.ncbi.nlm.nih.gov/geo/>). The expression profiling arrays of GSE99339 were generated applying GPL19109 [HG-U133_Plus_2] Affymetrix Human Genome U133 Plus 2.0 Array [CDF: Brainarray HG-U133-Plus2-Hs-ENTREZG_v18], including 15 Hypertensive Nephropathy specimens and 14 Tumor Nephrectomy specimens. The expression profiling arrays of GSE99325 were generated using GPL19184 [HG-U133A] Affymetrix Human Genome U133A Array [Custom Brainarray v18 ENTREZG CDF], including 20 Hypertensive Nephropathy specimens and 4 Cadaveric Donor specimens. Next, we used GPL570 [HG-U133_Plus_2] Affymetrix Human Genome U133 Plus 2.0 Array to generate the expression profiling arrays of GSE53757, including 72 ccRCC specimens and 72 normal specimens. Moreover, we also used GPL96 [HG-U133A] Affymetrix Human Genome U133A Array to generate the expression profiling arrays of GSE15641, including 49 RCC tissues and 23 normal tissues. We used the two gene expression profiles of GSE99339 and GSE99325 to filter differentially expressed genes (DEGs) of HN. Similarly, the two gene expression profiles of GSE53757 and GSE15641 were applied to filter DEGs of RCC. All procedures performed in this study were in accordance with the ethical standards of the institutional and/or national research committee and with the Helsinki Declaration (as revised in 2013).

Data processing

We used R packages of “affy”, “affyPLM”, and “limma” (<http://www.bioconductor.org/packages/release/bioc/html/affy.html>) to assess GSE99339, GSE99325, GSE53757 and GSE15641 RAW datasets. Background correction, probe summarization, quantile normalization, and log₂-transformation were used to generate a robust multi-array average (RMA), a log-transformed mismatch, and perfect match probe methods. We applied the Benjamini-Hochberg method to adjust original P values and the false discovery rate (FDR) procedure to calculate fold-changes (FC). We used Genes expression values of the $|\log_2 FC| > 1.5$ or < 0.667 and adjusted $P < 0.05$ to screen HN-DEGs. Moreover, we used the $|\log_2 FC| > 2$ or < 0.5 and adjusted $P < 0.05$ to filter

RCC-DEGs. Furthermore, volcano plots and Venn diagrams were made for co-DEGs of HN- and RCC-DEGs.

Analysis of protein-protein interaction (PPI) networks

We used the search tool for the retrieval of interacting genes (STRING) database (V11; <http://string-db.org/>) to analyze PPI networks of HN- and RCC-DEGs. Analytic data of the STRING database were downloaded with a combined score >0.4. Then we applied Cytoscape software (V3.5.1; <http://cytoscape.org/>) to analyze and visualize node degrees and biological networks.

Functional enrichment analysis

We conducted Gene Ontology (GO) and Kyoto Encyclopedia of Genes and Genomes (KEGG) pathway enrichment analysis of HN- and RCC-DEGs with the database for annotation, visualization and integrated discovery (DAVID) bioinformatics resources (<http://david.abcc.ncifcrf.gov/>). We identified the significantly enriched GO terms and KEGG pathway maps related to biofunctions based on a $P < 0.05$. Furthermore, we identified enriched functions of HN- and RCC-DEGs in molecular functions, biological processes, and cellular components, respectively.

Afterward, we used the AmiGO database (v2.0; <http://amigo.geneontology.org/amigo/>) to analyze the GO consortium of chosen co-DEGs in order to check the annotate and accuracy biofunctions of confirmed co-DEGs.

Identification of co-DEGs related to hypertension or renal cancer

We used the comparative toxicogenomics database (CTD, <http://ctdbase.org/>) to describe chemical-gene/protein interactions and chemical-disease and gene-disease relationships in order to know their associations. These data were used to identify the genes related to hypertension or renal cancer and scored genes indirectly through the CTD.

Co-DEGs validation

We used the Gene Expression Profiling Interactive Analysis (GEPIA) database (<http://gepia.cancer-pku.cn/>) to verify the differential expression of these genes in ccRCC. Overall survival curve was used to analyze survival differences.

Functional and pathway enrichment related to predicted miRNAs and Co-DEGs and validation of predicted miRNAs

We applied microRNA Data Integration Portal (mirDIP) (<http://ophid.utoronto.ca/mirDIP>) to predict miRNAs that may be regulated by 9 genes. Five top candidate miRNAs were determined according to predicted scores for each Co-DEG. We used Diana-miRPath (v3.0; <http://www.microrna.gr/miRPathv3>) to conduct GO terms and pathway enrichment analysis of these predicted miRNAs. Subsequently, the online tool Starbase (<http://starbase.sysu.edu.cn/>) was used to identify the relationship between predicted miRNAs and corresponding genes.

Statistical analysis

Data of DEGs were analyzed using R 4.0.0. Student's *t*-test was performed for comparisons between two groups, whereas ANOVA was performed for repeated measures. The χ^2 test was used to analyze the statistical significance of GO and pathway. Differences with $P < 0.05$ were considered statistically significant.

Data of Co-DEGs validation were based on GEPIA. We chose the dataset of KIRC. One-way ANOVA was used for differential analysis. The expression data were $\log_2(\text{TPM}+1)$ transformed for differential analysis and the $\log_2\text{FC}$ was defined as median (Tumor) – median (Normal). The screening criterion was P value < 0.05 . In survival analysis, we used Log-rank test for hypothesis test ($P < 0.05$). We calculated the hazards ratio (HR) based on Cox PH Mode and added the 95% CI as dotted line.

We used Pearson correlation analysis to identify the relationship between predicted miRNAs and Corresponding genes based on Starbase. The expression data of ccRCC were from TCGA. $P < 0.01$ was considered statistically significant.

Results

Identification of DEGs

21,592 probes in GSE99339 and GSE99325 datasets and 76,937 probes in GSE53757 and GSE15641 were identified. Then we confirmed HN- and RCC-DEGs. In GSE99325, we identified 1,147 DEGs in HN tissue specimens compared with normal tissue specimens, including 585 upregulated genes and 144 downregulated genes (*Figure 1A*). Similarly, we also described the DEGs of the other three datasets in the form of volcano plots (*Figure 1B,C,D*). The

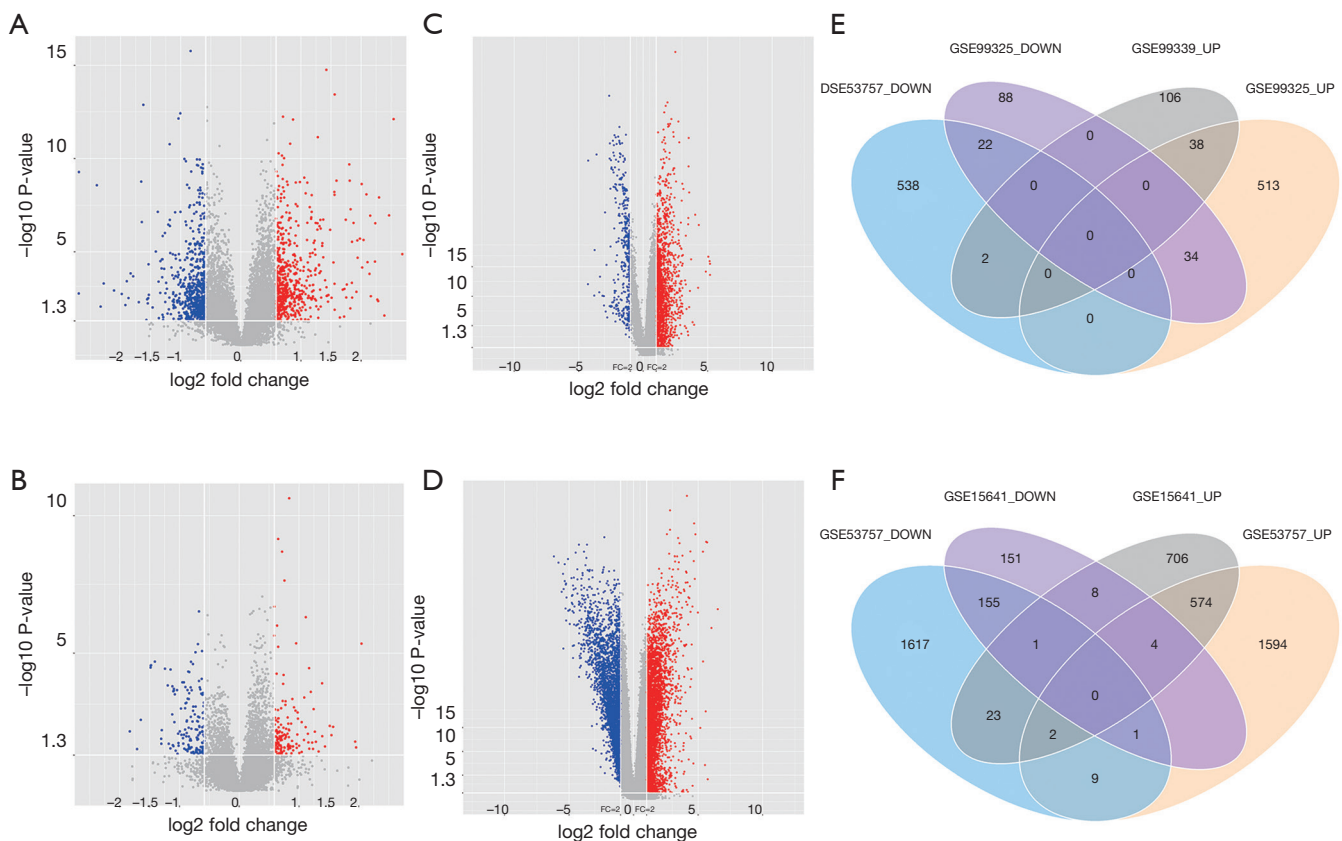


Figure 1 Volcano plots and Venn diagrams. (A-D) The volcano plots image the differentially expressed genes (DEGs) in GSE99325, GSE99339, GSE15641, and GSE53757. The blue and red dots represent downregulated and upregulated genes, respectively. (E) Venn diagrams of hypertensive nephrology (HN) related DEGs in GSE99325 and GSE99339. (F) Venn diagrams of renal cell carcinoma (RCC) related DEGs in GSE15641 and GSE53757. The purple and blue graphics represent downregulated genes. The grey and orange graphics represent upregulated genes.

common 60 genes of GSE99339 and GSE99325 were confirmed, including 38 upregulated and 22 downregulated genes, which are the DEGs of HN (Figure 1E). In the same way, the common 679 genes of GSE53757 and GSE15641 are the DEGs of RCC (Figure 1F). Heatmaps of HN-DEGs in relation to cellular response to tumor necrosis factor, response to lipopolysaccharide, multicellular organismal homeostasis and neutrophil degranulation were conducted for genes expression (Figure 2). The value of RCC-DEGs expression concerning extracellular structure organization, leukocyte migration, neutrophil activation and response to oxygen levels has been shown in Figure 3.

Functional enrichment in Co-DEGs

Figure 4A illustrates 9 Co-DEGs of HN- and RCC-

DEGs, including Sin3A associated protein 30 (*SAP30*), polymerase I and transcript release factor (*PTRF*), lysozyme (*LYZ*), PYD and CARD domain containing (*PYCARD*), estrogen related receptor gamma (*ESRRG*), coronin 1A (*CORO1A*), fibronectin 1 (*FNI*), branched chain amino acid transaminase 1 (*BCAT1*), cysteine rich protein 1 (*CRIP1*). We confirmed GO term enrichment concerning biological processes, molecular functions, and cellular components with AmiGO database. We found that Co-DEGs were related to many processes (Table S1).

PPI network analysis, GO analysis and KEGG pathway enrichment analysis

Fifty-eight and 618 nodes have been identified from PPI network of HN- and RCC-DEGs, respectively (Figure

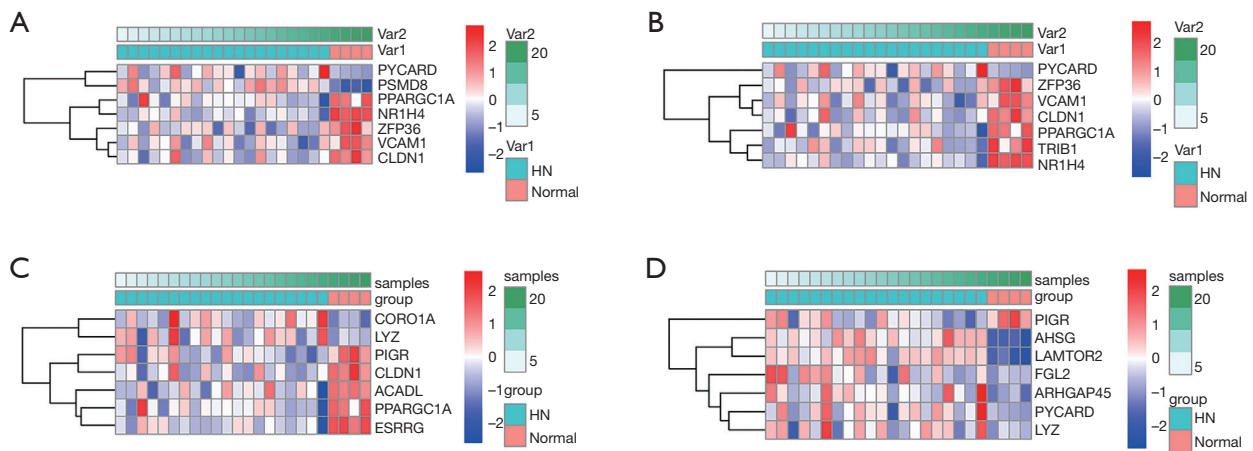


Figure 2 Heatmaps of hypertensive nephrology (HN) related differentially expressed genes (DEGs). (A-D) Results of DEGs expression concerning cellular response to tumor necrosis factor, response to lipopolysaccharide, multicellular organismal homeostasis, and neutrophil degranulation. Red, greater expression. Blue, less expression.

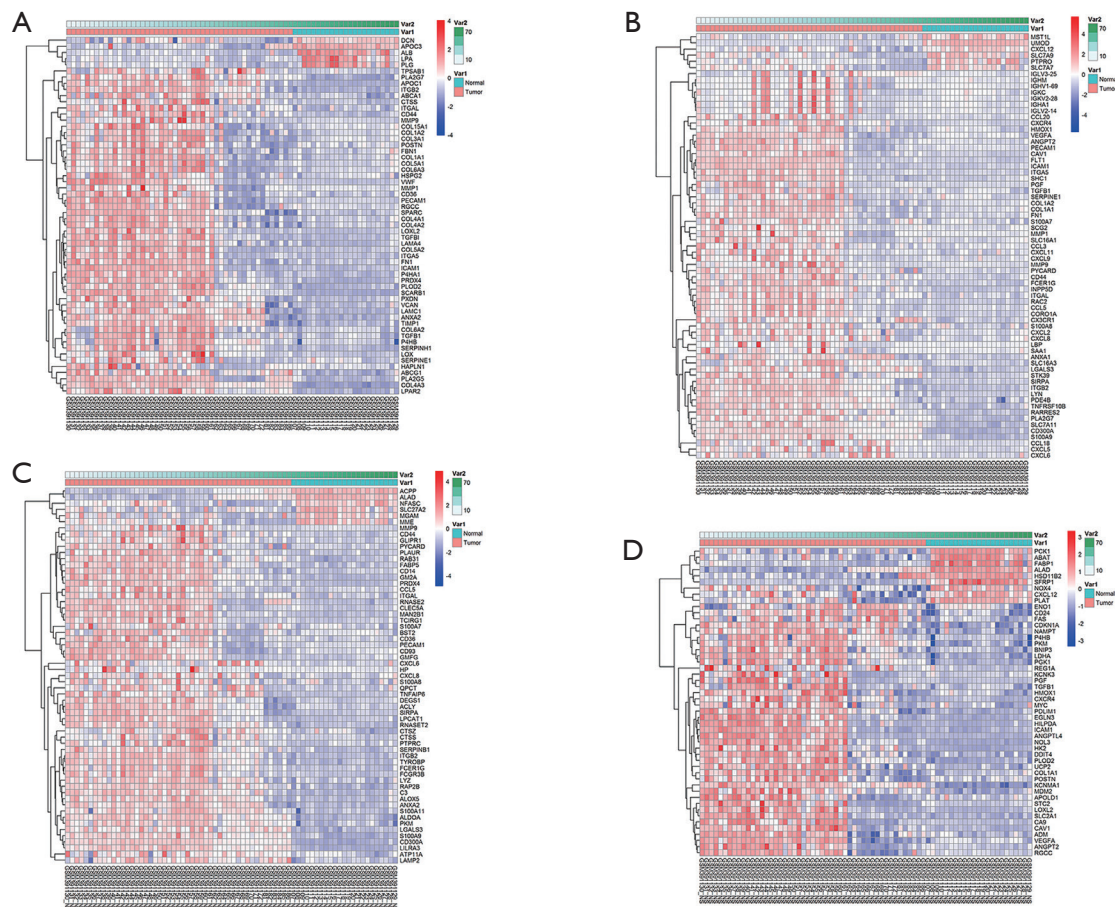


Figure 3 Heatmaps of renal cell carcinoma (RCC) related differentially expressed genes (DEGs). (A-D) Results of DEGs expression concerning extracellular structure organization, leukocyte migration, neutrophil activation and response to oxygen levels. Red, greater expression. Blue, less expression.

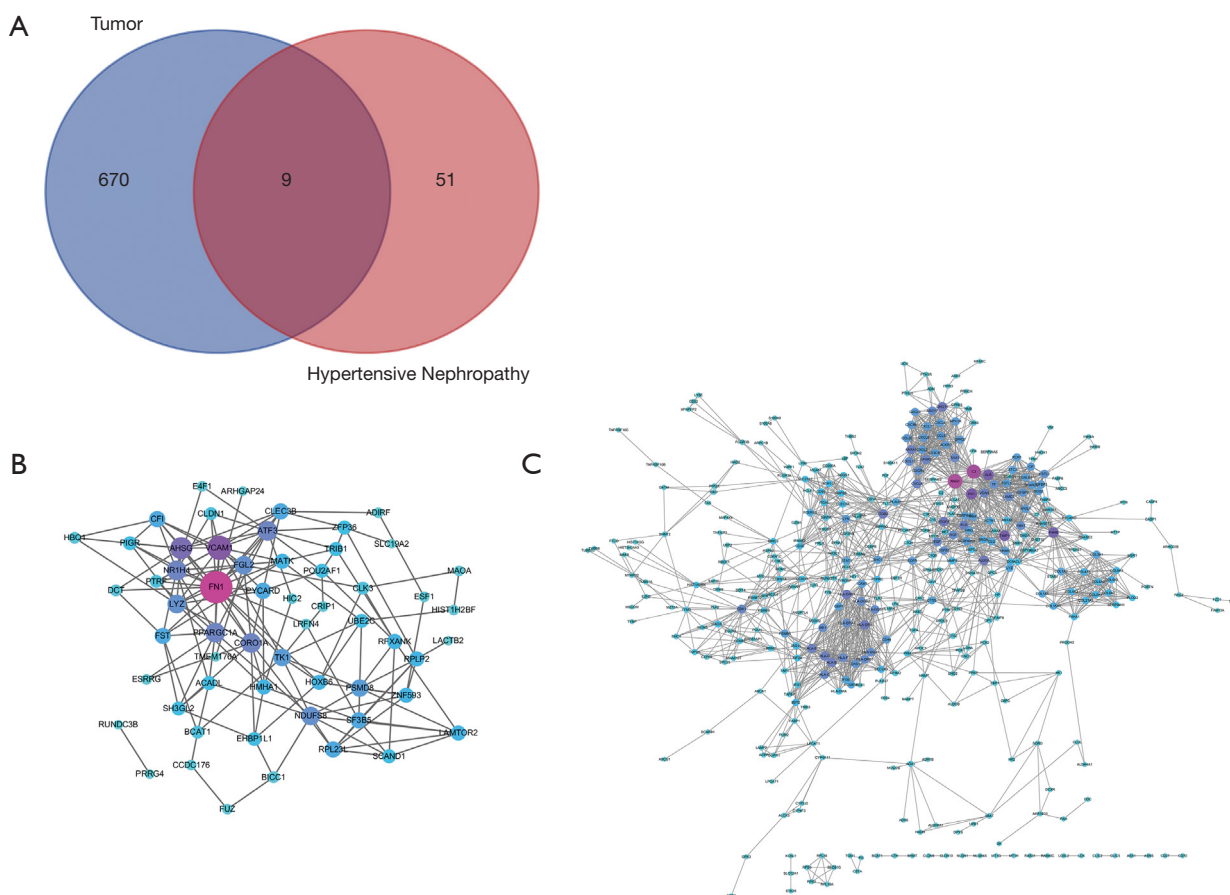


Figure 4 Venn diagrams and protein-protein interaction (PPI) network. (A) Common differentially expressed genes (DEGs) between renal cell carcinoma (RCC) and hypertensive nephropathy (HN); (B) PPI network of DEGs of HN; (C) PPI network of DEGs of RCC. Purple, greater degree. Blue, lesser degree.

4B,C). The hub nodes including fibronectin 1 (*FNI*; degree =21), vascular cell adhesion molecule 1 (*VCAM1*; degree =14), alpha 2-HS glycoprotein (*AHSG*; degree =12), nuclear receptor subfamily 1 group H member 4 (*NR1H4*; degree =10), PPARG coactivator 1 alpha (*PPARGC1A*; degree =10), coronin 1A (*CORO1A*; degree =10) and activating transcription factor 3 (*ATF3*; degree =10) are hub genes of HN. Similarly, the hub genes including kininogen 1 (*KNG1*; degree =58), complement C3 (*C3*; degree =55), fibronectin 1 (*FNI*; degree =38), TIMP metalloproteinase inhibitor 1 (*TIMP1*; degree =36), albumin (*ALB*; degree =36), prolyl 4-hydroxylase subunit beta (*P4HB*; degree =34) are illustrated in RCC-DEGs with a high degree.

We identified the GO terms involved in biological processes among HN-DEGs by using the DAVID database. They were mainly associated with cellular response to tumor necrosis factor (Fold Enrichment: 7.88; P value: 2.82E-05),

response to tumor necrosis factor (Fold Enrichment: 7.35; P value: 4.4E-05), response to lipopolysaccharide (Fold Enrichment: 6.95; P value: 6.26E-05), response to molecule of bacterial origin (Fold Enrichment: 6.68; P value: 7.98E-05) and cellular response to lipopolysaccharide (Fold Enrichment: 6.68; P value: 7.99E-05). There is evident correlation in secretory granule lumen (Fold Enrichment: 6.47; P value: 3.21E-04), cytoplasmic vesicle lumen (Fold Enrichment: 6.14; P value: 4.22E-04), vesicle lumen (Fold Enrichment: 6.12; P value: 4.29E-04) and cytosolic part (Fold Enrichment: 7.00; P value: 7.30E-04) in connection with cellular components. Furthermore, the terms concerning molecular functions were primarily referred to primary amine oxidase activity (Fold Enrichment: 107.25; P value: 1.41E-04), transcription coregulator activity (Fold Enrichment: 4.58; P value: 3.22E-04) and oxidoreductase activity, acting on the CH-NH2 group of donors, oxygen

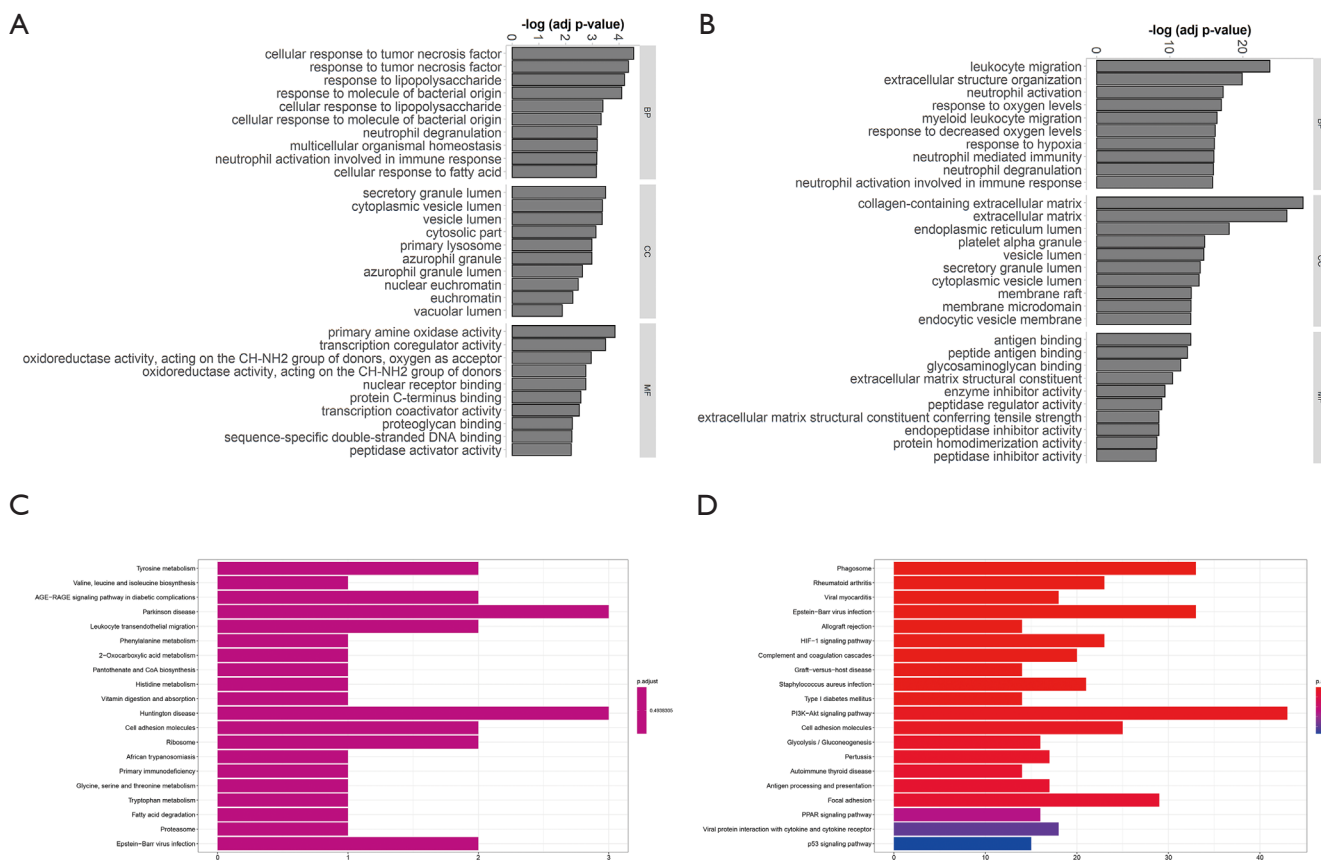


Figure 5 Gene Ontology (GO) and Kyoto Encyclopedia of Genes and Genomes (KEGG) pathway enrichment analysis. (A,B) Hypertensive nephrology and renal cell carcinoma related GO analysis for differentially expressed genes (DEGs). The ordinates represent the function name of the DEGs, and the abscissas represent negative Lg-P values. (C,D) KEGG pathway of hypertensive nephrology and renal cell carcinoma related DEGs. Rectangular length and rectangular colors represent the number of DEGs contained in the pathway and P. adjust, respectively.

as acceptor (Fold Enrichment: 40.22; P value: 0.001). RCC was also analyzed. The biological processes terms including leukocyte migration (Fold Enrichment: 4.19; P value: 2.13E-24), extracellular structure organization (Fold Enrichment: 4.19; P value: 1.28E-20), neutrophil activation (Fold Enrichment: 3.56; P value: 4.95E-18) and response to oxygen levels (Fold Enrichment: 4.16; P value: 8.77E-20) were significantly enriched. Similarly, the terms of collagen-containing extracellular matrix (Fold Enrichment: 5.60; P value: 5.73E-29), extracellular matrix (Fold Enrichment: 4.41; P value: 9.82E-27) and endoplasmic reticulum lumen (Fold Enrichment: 4.69; P value: 7.46E-19) concerning cellular components were primarily enriched. In addition, the molecular functions terms of antigen binding (Fold Enrichment: 4.66; P value:

1.38E-13), peptide antigen binding (Fold Enrichment: 13.10; P value: 3.94E-13) and glycosaminoglycan binding (Fold Enrichment: 4.17; P value: 3.20E-12) were notably enriched (Figure 5A,B).

KEGG pathway analysis data is shown in Figure 5. It indicated that the HN-DEGs were greatly enriched in pathways of tyrosine metabolism (P value: 0.006) (Figure 5C). However, KEGG terms including phagosome (P value: 6.96E-13), rheumatoid arthritis (P value: 1.48E-10) and viral myocarditis (P value: 5.03E-10) were enriched in RCC-DEGs (Figure 5D).

Co-DEGs validation and detection

The CTD showed that Co-DEGs *BCAT1*, *CORO1A*,

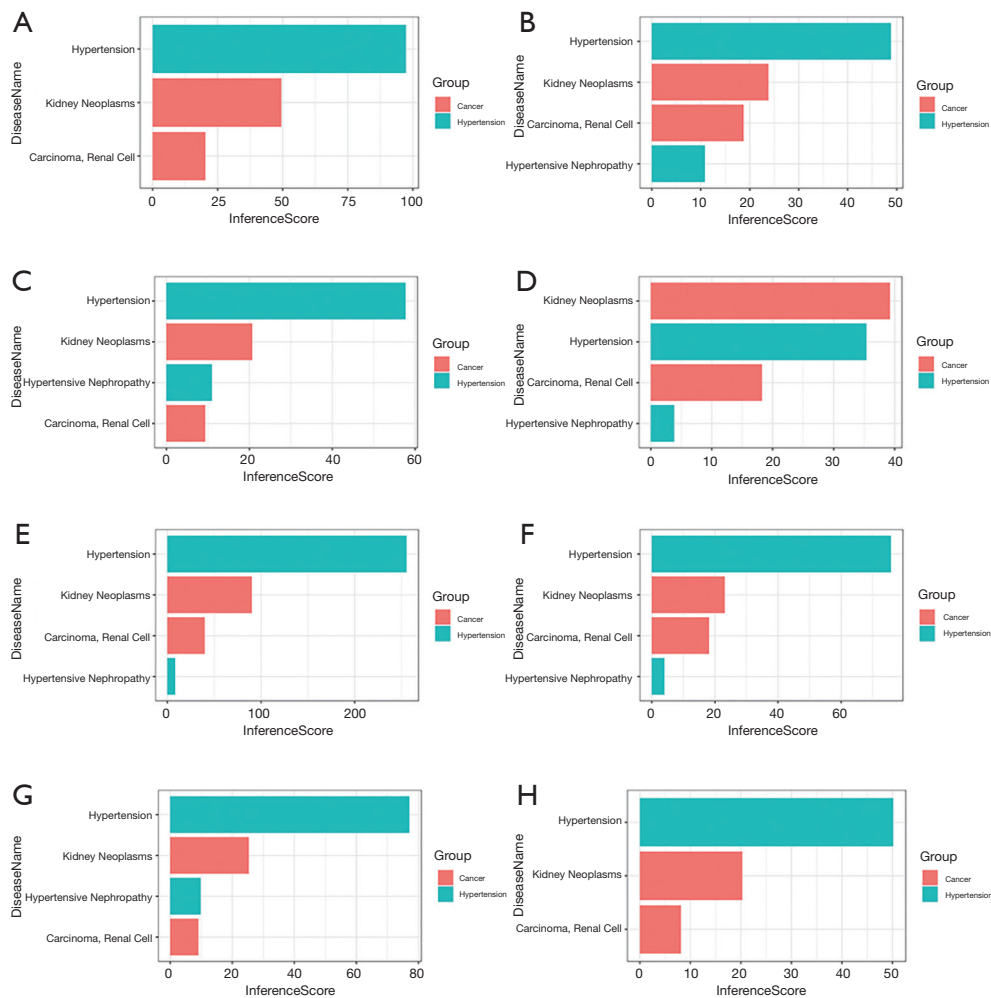


Figure 6 Co-expressed genes related to hypertension and kidney cancer based on the comparative toxicogenomics database (CTD). (A-H) Inference Score of *BCAT1*, *CORO1A*, *CRIP1*, *ESRRG*, *FN1*, *LYZ*, *PYCARD*, *SAP30*.

CRIP1, *ESRRG*, *FN1*, *LYZ*, *PYCARD*, and *SAP30* targeted hypertension and renal cancer and these data appear in *Figure 6*. Compared with para cancerous normal tissues, the expression levels of 7 genes except *BCAT1* were obviously higher in ccRCC in view of the GEPIA database (*Figure 7A,B,C,D,E,F,G,H*). Among the 8 key genes, we found that *CRIP1*, *ESRRG*, *LYZ*, and *PYCARD* were obviously associated with the overall survival of ccRCC patients (*Figure 7I,J,K,L*).

Functional and pathway enrichment related to predicted miRNAs and Co-DEGs and validation of predicted miRNAs

We used mirDIP and DIANA-MirPath database to

predict the top 5 targeted miRNAs of each Co-DEG associated with HN-related RCC (*Table S2*). In *Figure 8*, we identified the relationship between predicted miRNAs and Corresponding genes in ccRCC. Hsa-miR-429 and hsa-miR-200b-3p are negatively correlated with *FN1*, respectively. Hsa-miR-30e-5p and hsa-miR-30b-5p are negatively correlated with *SAP30*, respectively. Hsa-miR-221-5p is negatively correlated with *CRIP1*. Hsa-miR-205-5p, hsa-miR-152-3p and hsa-miR-137 are negatively correlated with *ESRRG*, respectively.

Discussion

Numerous observational studies have systematically reported an increased risk of RCC in patients with

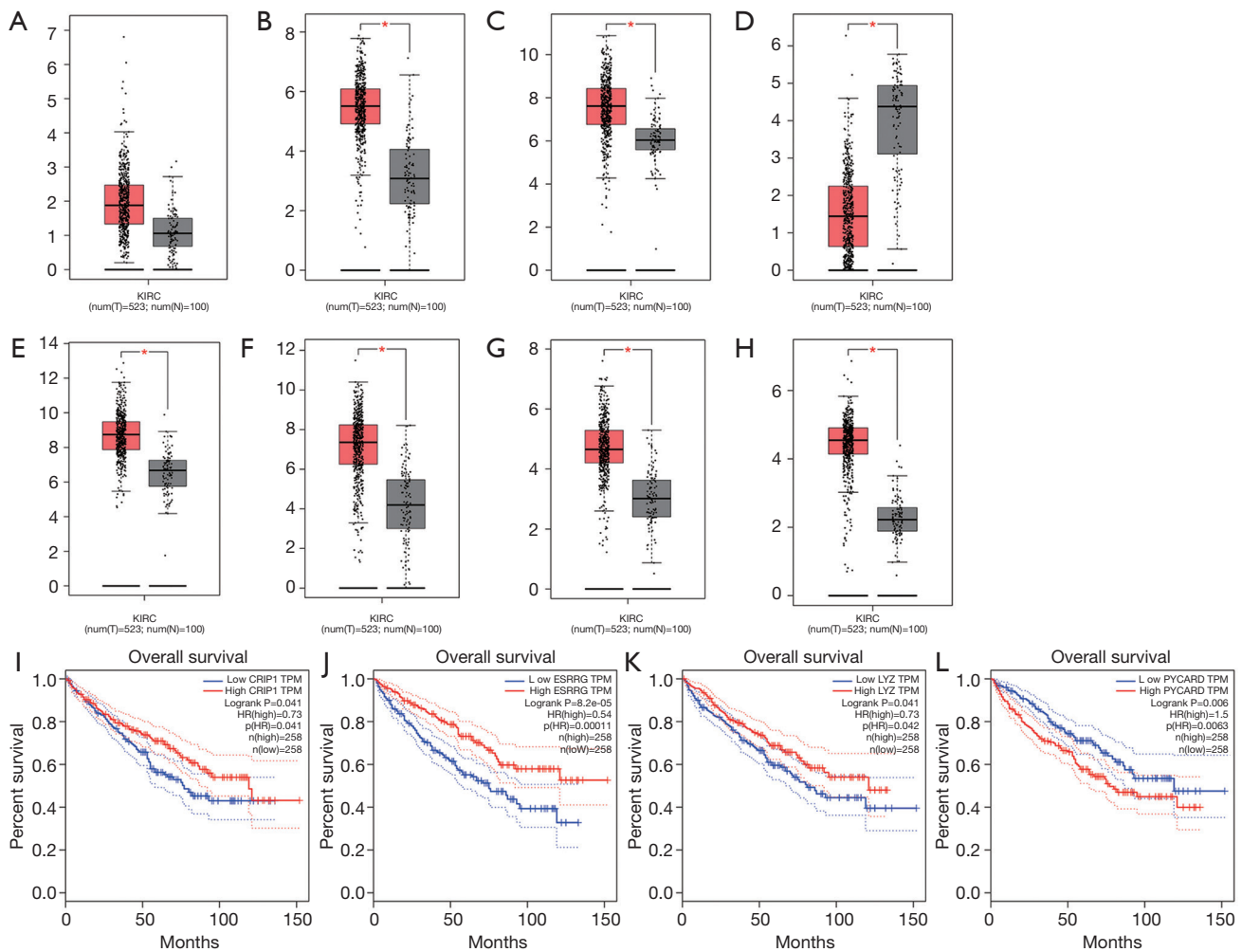


Figure 7 Gene expression and overall survival based on GEPIA database. (A-H) The gene expression levels of *BCAT1*, *CORO1A*, *CRIP1*, *ESRRG*, *FN1*, *LYZ*, *PYCARD* and *SAP30* in normal kidney and renal clear cell carcinoma (ccRCC) tissues. (I-L) Overall survival analysis of 4 genes in ccRCC. Expression levels of *CRIP1*, *ESRRG*, *LYZ* and *PYCARD* are associated with the overall survival of patients with ccRCC based on $P < 0.05$.

hypertension (17,18). The biological mechanism of the relationship between hypertension and RCC is indefinite. However, it is speculated that it is related to chronic kidney hypoxia and lipid peroxidation with the generation of reactive oxygen species (ROS) (19,20). Patients with hypertension may cause chronic kidney hypoxia due to the transcription of hypoxia inducible factors, which can promote tumor cell angiogenesis and proliferation (21). we identified 8 key genes of hypertension-related RCC, including *BCAT1*, *CORO1A*, *CRIP1*, *ESRRG*, *FN1*, *LYZ*, *PYCARD*, and *SAP30*. These genes will help us further explore the mechanism of hypertension-related RCC and

may become biomarkers of hypertension-related RCC. And they are also important for exploring new therapeutic targets of hypertension-related RCC.

One study showed that *CRIP1* has a strong connection with pressure at the population level. The effect of *CRIP1* on blood pressure may be achieved by mediating *SH2B3* (22). Meanwhile, Macrophages that lack *SH2B3* expression are easily activated, producing more ROS (23), which can cause kidney injury. We generally believe that *SH2B3* negatively inhibits proinflammatory cell signaling within the kidney in normal and pathological states (24). Long-term effects of these mechanisms may lead to the development of

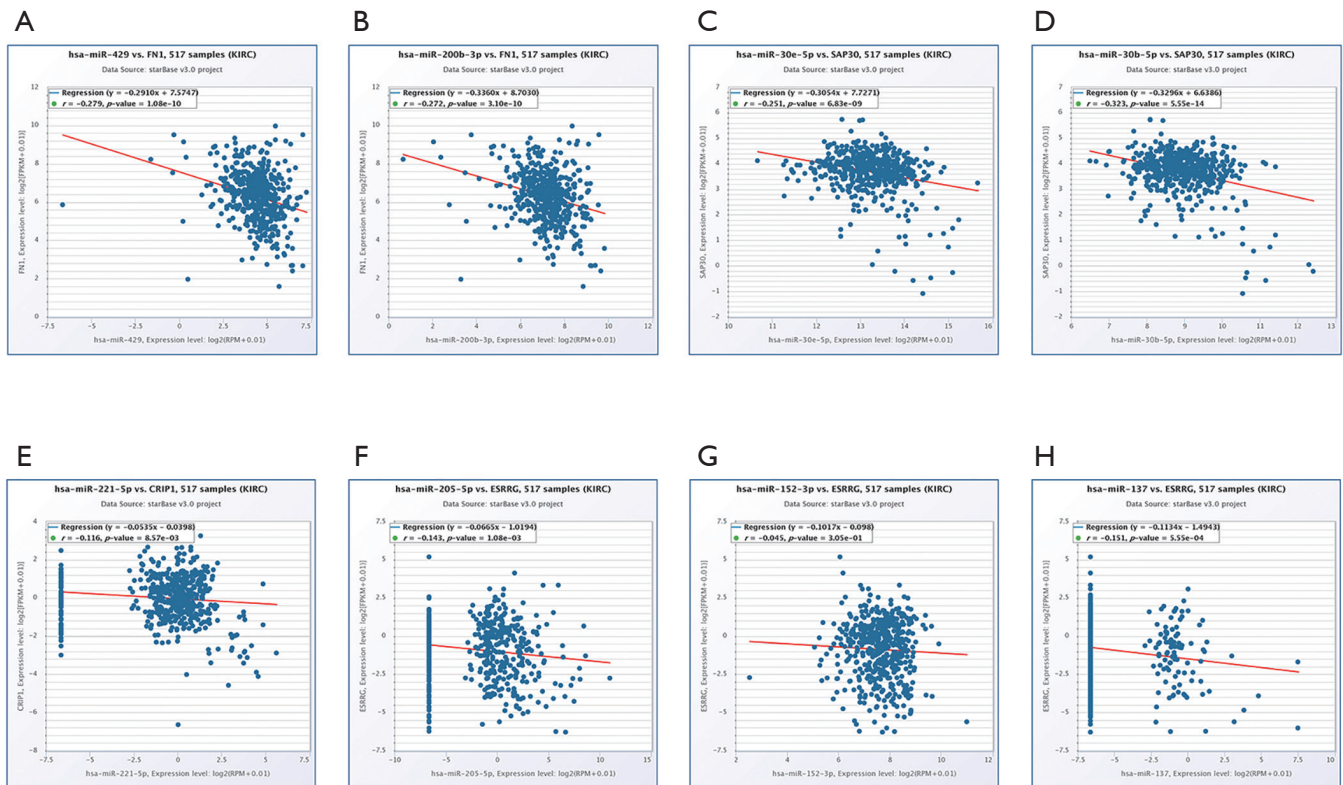


Figure 8 The relationship between predicted miRNAs and Corresponding genes. The relative expression levels between predicted miRNAs and Corresponding genes in renal clear cell carcinoma in starBase. (A,B) Hsa-miR-429 and hsa-miR-200b-3p are negatively correlated with FN1, respectively ($P < 0.01$). (C,D) Hsa-miR-30e-5p and hsa-miR-30b-5p are negatively correlated with SAP30, respectively ($P < 0.01$). (E) Hsa-miR-221-5p is negatively correlated with CRIP1 ($P < 0.01$). (F-H) Hsa-miR-205-5p, hsa-miR-152-3p and hsa-miR-137 are negatively correlated with ESRRG, respectively ($P < 0.01$).

hypertension-related RCC. The detection of *CRIP1* helps us to detect RCC early in patients with hypertension, so as to improve the survival rate of RCC. Recent studies have revealed that *ESRRG* is a key transcriptional regulator of mitochondrial oxidative phosphorylation (OxPhos) and fatty acid oxidation (FAO) (25). Through the analysis of epigenomic elements of the promoter, it is found that *ESRRG* is a new obesity-susceptibility gene (26). It is well known that obesity and hypertension are highly correlated. Based on this, we speculate that *ESRRG* is associated with hypertension. *ESRRG* is highly expressed in the kidney and plays a major role in normal embryonic kidney development (27). The lack of *ESRRG* in renal epithelial cells (RECs) causes serious renal energy and absorption dysfunction and renal failure. The expression of *ESRRG* is positively correlated with renal function and decreases in patients with chronic kidney disease (CKD) (28). CKD is one of the causes of RCC (29). *ESRRG* and *ESRRG* drive changes in HIF1A

and HIF2A, which are important in developing ccRCC molecular phenotypes (30). In addition, *ESRRG* also plays a role in other tumors, including breast cancer, endometrial cancer, gastric cancer, liver cancer, and prostate cancer. Further exploration of the role of *ESRRG* in the occurrence and development of hypertension-related RCC will help us find new therapeutic targets for RCC, thereby alleviating the situation of drug resistance in the treatment of renal cancer. *FN1* is a gene that has been widely explored. The expression of *FN1* is increased in patients with hypertension (31). Several studies show a strong correlation between *FN1* and RCC (32,33). *FN1* expression in RCC is related to a higher disease-related mortality rate, indicating a probable role in RCC progression (34). Apoptosis genes such as *PYCARD* have shown potential to improve the prognosis of other cancers and may be demonstrated by further research to have the same potential in RCC (35). Transcription factor *SAP30* is important to activation of expression of *NETO2*

gene in ccRCC. Meanwhile, mRNA level of *SAP30* increased significantly and was positively correlated with *NETO2* gene expression (36).

In our data, miR-429, miR-200b-3p, miR-30e-5p, miR-30b-5p, miR-221-5p, miR-205-5p, miR-152-3p and miR-137 may sponge with corresponding genes and act on hypertension-related RCC. Has-miR-429 is one of the most studied miRNAs in RCC. It is reported that miR-429 suppresses tumor cell proliferation, metastasis and epithelial-mesenchymal transition by direct targeting of *BMI1*, *E2F3* and *VEGF* in RCC (37,38). MiR-137 inhibits the growth and invasion of ccRCC cells, and induces apoptosis, acting as a tumor suppressor gene. MiR-137 works by targeting 3'-UTR of *RLIP76* which is an oncogene identified in ccRCC (39).

Conclusions

According to existing literature reports, several genes such as *CRIP1*, *ESRRG*, *FN1*, *PYCARD*, and *SAP30* are related to hypertension or RCC. Through the verification of CTD, GEPIA and Starbase databases, we found that the two genes *CRIP1*, *ESRRG* and their corresponding predicted miRNAs are most likely instructive for further exploration of hypertension-related RCC and contribute to finding new therapeutic targets.

However, some limitations also exist. primarily, this is a microarray analysis study and our data were acquired from a publicly available database. Given that gene expression is not necessarily equivalent to protein expression, we need further *in vivo* and *in vitro* experiments to clarify molecular mechanisms of key genes for clinical applications. Secondly, prospective clinical studies may validate our point of view better.

Acknowledgments

Funding: This work was supported by research grants from the Natural Science Foundation of China (no. 81972393, 81772705, 31570775).

Footnote

Reporting Checklist: The authors have completed the MDAR reporting checklist. Available at <http://dx.doi.org/10.21037/tau-20-817>

Conflicts of Interest: All authors have completed the ICMJE

uniform disclosure form (available at <http://dx.doi.org/10.21037/tau-20-817>). The authors have no conflicts of interest to declare.

Ethical Statement: The authors are accountable for all aspects of the work in ensuring that questions related to the accuracy or integrity of any part of the work are appropriately investigated and resolved. All procedures performed in this study were in accordance with the ethical standards of the institutional and/or national research committee and with the Helsinki Declaration (as revised in 2013).

Open Access Statement: This is an Open Access article distributed in accordance with the Creative Commons Attribution-NonCommercial-NoDerivs 4.0 International License (CC BY-NC-ND 4.0), which permits the non-commercial replication and distribution of the article with the strict proviso that no changes or edits are made and the original work is properly cited (including links to both the formal publication through the relevant DOI and the license). See: <https://creativecommons.org/licenses/by-nc-nd/4.0/>.

References

1. Saad AM, Gad MM, Al-Husseini MJ, et al. Trends in Renal-Cell Carcinoma Incidence and Mortality in the United States in the Last 2 Decades: A SEER-Based Study. *Clin Genitourin Cancer* 2019;17:46-57.e5.
2. Znaor A, Lortet-Tieulent J, Laversanne M, et al. International variations and trends in renal cell carcinoma incidence and mortality. *Eur Urol* 2015;67:519-30.
3. Siegel RL, Miller KD, Jemal A. Cancer statistics, 2020. *CA: a cancer journal for clinicians* 2020;70:7-30.
4. Chen W, Sun K, Zheng R, et al. Cancer incidence and mortality in China, 2014. *Chin J Cancer Res* 2018;30:1-12.
5. Ljungberg B, Bensalah K, Canfield S, et al. EAU guidelines on renal cell carcinoma: 2014 update. *Eur Urol* 2015;67:913-24.
6. Zhang X, Ren J, Yan L, et al. Cytoplasmic expression of pontin in renal cell carcinoma correlates with tumor invasion, metastasis and patients' survival. *PLoS One* 2015;10:e0118659.
7. Di Pietro G, Luu HN, Spiess PE, et al. Biomarkers and new therapeutic targets in renal cell carcinoma. *Eur Rev Med Pharmacol Sci* 2018;22:5874-91.
8. Chen W, Hill H, Christie A, et al. Targeting renal cell carcinoma with a HIF-2 antagonist. *Nature*

- 2016;539:112-7.
9. Morais C, Gobe G, Johnson DW, et al. The emerging role of nuclear factor kappa B in renal cell carcinoma. *Int J Biochem Cell Biol* 2011;43:1537-49.
 10. Kearney PM, Whelton M, Reynolds K, et al. Global burden of hypertension: analysis of worldwide data. *Lancet* 2005;365:217-23.
 11. Radišauskas R, Kuzmickiene I, Milinaviciene E, et al. Hypertension, serum lipids and cancer risk: A review of epidemiological evidence. *Medicina (Kaunas)* 2016;52:89-98.
 12. Shen T, Shu XO, Xiang YB, et al. Association of hypertension and obesity with renal cell carcinoma risk: a report from the Shanghai Men's and Women's Health Studies. *Cancer Causes Control* 2015;26:1173-80.
 13. Hofmann JN, Corley DA, Zhao WK, et al. Chronic kidney disease and risk of renal cell carcinoma: differences by race. *Epidemiology* 2015;26:59-67.
 14. Mariusdottir E, Ingimarsson JP, Jonsson E, et al. Occupation as a risk factor for renal cell cancer: a nationwide, prospective epidemiological study. *Scand J Urol* 2016;50:181-5.
 15. Macleod LC, Hotaling JM, Wright JL, et al. Risk factors for renal cell carcinoma in the VITAL study. *J Urol* 2013;190:1657-61.
 16. Hidayat K, Du X, Zou SY, et al. Blood pressure and kidney cancer risk: meta-analysis of prospective studies. *J Hypertens* 2017;35:1333-44.
 17. Chow WH, Gridley G, Fraumeni JF, Jr., et al. Obesity, hypertension, and the risk of kidney cancer in men. *N Engl J Med* 2000;343:1305-11.
 18. Choi MY, Jee SH, Sull JW, et al. The effect of hypertension on the risk for kidney cancer in Korean men. *Kidney Int* 2005;67:647-52.
 19. Sharifi N, Farrar WL. Perturbations in hypoxia detection: a shared link between hereditary and sporadic tumor formation? *Med Hypotheses* 2006;66:732-5.
 20. Gago-Dominguez M, Castela JE, Yuan JM, et al. Lipid peroxidation: a novel and unifying concept of the etiology of renal cell carcinoma (United States). *Cancer Causes Control* 2002;13:287-93.
 21. Kaelin WG Jr. The von Hippel-Lindau gene, kidney cancer, and oxygen sensing. *J Am Soc Nephrol* 2003;14:2703-11.
 22. Zeller T, Schurmann C, Schramm K, et al. Transcriptome-Wide Analysis Identifies Novel Associations With Blood Pressure. *Hypertension* 2017;70:743-50.
 23. Gueller S, Goodridge HS, Niebuhr B, et al. Adaptor protein Lnk inhibits c-Fms-mediated macrophage function. *J Leukoc Biol* 2010;88:699-706.
 24. Blass G, Mattson DL, Staruschenko A. The function of SH2B3 (LNK) in the kidney. *Am J Physiol Renal Physiol* 2016;311:F682-5.
 25. Eichner LJ, Giguere V. Estrogen related receptors (ERRs): a new dawn in transcriptional control of mitochondrial gene networks. *Mitochondrion* 2011;11:544-52.
 26. Dong SS, Guo Y, Zhu DL, et al. Epigenomic elements analyses for promoters identify ESRRG as a new susceptibility gene for obesity-related traits. *Int J Obes (Lond)* 2016;40:1170-6.
 27. Berry R, Harewood L, Pei L, et al. Esrrg functions in early branch generation of the ureteric bud and is essential for normal development of the renal papilla. *Hum Mol Genet* 2011;20:917-26.
 28. Zhao J, Lupino K, Wilkins BJ, et al. Genomic integration of ERRgamma-HNF1beta regulates renal bioenergetics and prevents chronic kidney disease. *Proc Natl Acad Sci U S A* 2018;115:E4910-9.
 29. Hofmann JN, Purdue MP. CKD and risk of renal cell carcinoma: a causal association? *J Am Soc Nephrol* 2014;25:2147-8.
 30. Neely BA, Wilkins CE, Marlow LA, et al. Proteotranscriptomic Analysis Reveals Stage Specific Changes in the Molecular Landscape of Clear-Cell Renal Cell Carcinoma. *PLoS One* 2016;11:e0154074.
 31. Stoynev N, Dimova I, Rukova B, et al. Gene expression in peripheral blood of patients with hypertension and patients with type 2 diabetes. *J Cardiovasc Med (Hagerstown)* 2014;15:702-9.
 32. Waalkes S, Atschekzei F, Kramer MW, et al. Fibronectin 1 mRNA expression correlates with advanced disease in renal cancer. *BMC Cancer* 2010;10:503.
 33. Song E, Song W, Ren M, et al. Identification of potential crucial genes associated with carcinogenesis of clear cell renal cell carcinoma. *J Cell Biochem* 2018;119:5163-74.
 34. Steffens S, Schrader AJ, Vetter G, et al. Fibronectin 1 protein expression in clear cell renal cell carcinoma. *Oncol Lett* 2012;3:787-90.
 35. Rajandram R, Pat BK, Li J, et al. Expression of apoptotic tumour necrosis factor receptor-associated factor, caspase recruitment domain and cell death-inducing DFF-45 effector genes in therapy-treated renal cell carcinoma. *Nephrology (Carlton)* 2009;14:205-12.
 36. Snezhkina AV, Nyushko KM, Zaretsky AR, et al. Transcription Factor SAP30 Is Involved in the Activation of NETO2 Gene Expression in Clear Cell Renal Cell

- Carcinoma. *Mol Biol (Mosk)* 2018;52:451-9.
37. Qiu M, Liang Z, Chen L, et al. MicroRNA-429 suppresses cell proliferation, epithelial-mesenchymal transition, and metastasis by direct targeting of BMI1 and E2F3 in renal cell carcinoma. *Urol Oncol* 2015;33:332.e9-e18.
38. Chen D, Li Y, Li Y, et al. Tumor suppressive microRNA429 regulates cellular function by targeting VEGF in clear cell renal cell carcinoma. *Mol Med Rep* 2016;13:1361-6.
39. Wang M, Gao H, Qu H, et al. MiR-137 suppresses tumor growth and metastasis in clear cell renal cell carcinoma. *Pharmacol Rep* 2018;70:963-71.

Cite this article as: Huang W, Wu K, Wu R, Chen Z, Zhai W, Zheng J. Bioinformatic gene analysis for possible biomarkers and therapeutic targets of hypertension-related renal cell carcinoma. *Transl Androl Urol* 2020;9(6):2675-2687. doi: 10.21037/tau-20-817

Table S1 The Gene Ontology (GO) analysis of the co-expressed differential genes of hypertension-related renal cell carcinoma

Gene	GO class (direct)	Evidence	Evidence with	Reference	
BCAT1	G1/S transition of mitotic cell cycle	TAS		PMID:8692959	
	cytosol	TAS		Reactome: R-HSA-508189	
	branched-chain amino acid biosynthetic process	TAS		PMID:6933702	
	branched-chain amino acid catabolic process	TAS		Reactome: R-HSA-70895	
	identical protein binding	IEA	UniProtKB: P54690 ensembl: ENSRNOP0000021193	GO_REF:0000107	
	L-leucine transaminase activity	IEA	EC:2.6.1.42	GO_REF:0000003	
	L-valine transaminase activity	IEA	EC:2.6.1.42	GO_REF:0000003	
	L-isoleucine transaminase activity	IEA	EC:2.6.1.42	GO_REF:0000003	
	valine biosynthetic process	IBA	PANTHER: PTN000214538 PomBase: SPBC428.02c	PMID:21873635	
	mitochondrion	IBA	MGI: MGI:1276534 PANTHER: PTN000214537 PomBase: SPBC428.02c RGD:68948 SGD: S000001251 UniProtKB: O15382	PMID:21873635	
	branched-chain-amino-acid transaminase activity	IBA	MGI: MGI:104861 MGI: MGI:1276534 PANTHER: PTN000214538 PomBase: SPBC428.02c RGD:2195 RGD:68948 SGD: S000001251 SGD: S000003909	PMID:21873635	
	leucine biosynthetic process	IBA	PANTHER: PTN000214538 PomBase: SPBC428.02c RGD:68948	PMID:21873635	
	CORO1A	immunological synapse	IDA		PMID:24760828
		phagolysosome assembly	IMP		PMID:12132654
phagocytic cup		IDA		PMID:17442961	
RNA binding		HDA		PMID:22658674	
actin binding		IPI	UniProtKB: P60709	PMID:23100250	
actin monomer binding		IMP		PMID:23100250	
protein binding		IPI	UniProtKB: P14598	PMID:11094157	
cytoplasm		IDA		PMID:17341475	
early endosome		IEA	UniProtKB: O89053 ensembl: ENSMUSP00000101972	GO_REF:0000107	
cytosol		IEA	GO:0061502	GO_REF:0000108	
actin filament		IDA		PMID:15800061	
plasma membrane		IDA		PMID:17341475	
cell-cell junction		IEA	UniProtKB: O89053 ensembl: ENSMUSP00000101972	GO_REF:0000107	
calcium ion transport		IEA	UniProtKB: O89053 ensembl: ENSMUSP00000101972	GO_REF:0000107	
phagocytosis		IMP		PMID:17442961	
protein C-terminus binding		IPI	UniProtKB: Q15080	PMID:9365277	
cytoskeletal protein binding		ISS	UniProtKB: O89053	GO_REF:0000024	
regulation of cell shape		IEA	UniProtKB: O89053 ensembl: ENSMUSP00000101972	GO_REF:0000107	
membrane		HDA		PMID:19946888	
lamellipodium		IDA		PMID:17442961	
actin cytoskeleton organization		IMP		PMID:17442961	
positive regulation of cell migration		IEA	UniProtKB: O89053 ensembl: ENSMUSP00000101972	GO_REF:0000107	

	axon	IEA	UniProtKB: O89053 ensembl: ENSMUSP00000101972	GO_REF:0000107
	leukocyte chemotaxis	IEA	UniProtKB: O89053 ensembl: ENSMUSP00000101972	GO_REF:0000107
	phagocytic vesicle membrane	IEA	UniProtKB-SubCell:SL-0205	GO_REF:0000039
	cortical actin cytoskeleton	IDA		PMID:15800061
	negative regulation of vesicle fusion	IEA	UniProtKB: O89053 ensembl: ENSMUSP00000101972	GO_REF:0000107
	cell-substrate adhesion	IMP		PMID:17442961
	myosin heavy chain binding	IPI	UniProtKB: P35579	PMID:23100250
	uropod organization	IEA	UniProtKB: O89053 ensembl: ENSMUSP00000101972	GO_REF:0000107
	regulation of actin cytoskeleton organization	IMP		PMID:24760828
	protein-containing complex	IDA		PMID:11094157
	nerve growth factor signaling pathway	IEA	UniProtKB: O89053 ensembl: ENSMUSP00000101972	GO_REF:0000107
	positive regulation of T cell proliferation	IEA	UniProtKB: O89053 ensembl: ENSMUSP00000101972	GO_REF:0000107
	protein homodimerization activity	IDA		PMID:15601263
	T cell homeostasis	IEA	UniProtKB: O89053 ensembl: ENSMUSP00000101972	GO_REF:0000107
	natural killer cell degranulation	IMP		PMID:24760828
	negative regulation of neuron apoptotic process	IEA	UniProtKB: O89053 ensembl: ENSMUSP00000101972	GO_REF:0000107
	phosphatidylinositol 3-kinase binding	IDA		PMID:11094157
	innate immune response	NAS		PMID:17341475
	phagocytic vesicle	IDA		PMID:17442961
	homeostasis of number of cells within a tissue	IEA	UniProtKB: O89053 ensembl: ENSMUSP00000101972	GO_REF:0000107
	positive chemotaxis	IDA		PMID:17442961
	actin filament binding	IDA		PMID:15601263
	negative regulation of actin nucleation	IDA		PMID:17442961
	regulation of release of sequestered calcium ion into cytosol	IEA	UniProtKB: O89053 ensembl: ENSMUSP00000101972	GO_REF:0000107
	early endosome to recycling endosome transport	IEA	UniProtKB: O89053 ensembl: ENSMUSP00000101972	GO_REF:0000107
	extracellular exosome	HDA		PMID:20458337
	cellular response to interleukin-4	IEA	UniProtKB: O89053 ensembl: ENSMUSP00000101972	GO_REF:0000107
	glutamatergic synapse	IEA	UniProtKB: O89053 ensembl: ENSMUSP00000101972	GO_REF:0000107
	cortical actin cytoskeleton	IDA		PMID:24760828
	actin filament binding	IBA	FB: FBgn0029903 MG: MGI:1345961 PANTHER: PTN000091698 SGD: S000004421 UniProtKB: P31146 UniProtKB: Q9BR76 UniProtKB: Q9ULV4 WB: WBGene00004075 dictyBase: DDB_G0267382 dictyBase: DDB_G0269388	PMID:21873635
	actin filament organization	IBA	MG: MGI:1345961 MG: MGI:1926135 PANTHER: PTN000091698 SGD: S000004421 UniProtKB: P57737 UniProtKB: Q9BR76 dictyBase: DDB_G0267382	PMID:21873635

	cell migration	IBA	MGI:1345961 PANTHER: PTN000091809 UniProtKB: Q9BR76 UniProtKB: Q9ULV4 ZFIN: ZDB-GENE-030114-6	PMID:21873635
CRIP1	AT DNA binding	IDA		PMID:20108983
	cytoplasm	IDA		PMID:20415737
	immune response	IEP		PMID:20415737
	heart development	TAS		PMID:7999070
	zinc ion binding	IDA		PMID:9126610
	DNA binding, bending	IDA		PMID:20108983
	intrinsic apoptotic signaling pathway in response to DNA damage	IDA		PMID:20415737
	response to organic substance	IEP		PMID:17486081
	response to zinc ion	IDA		PMID:7999070
	regulation of gene expression	IEP		PMID:7999070
	peptide binding	IDA		PMID:18670594
	prostate gland stromal morphogenesis	IEP		PMID:9507743
	cellular response to antibiotic	IDA		PMID:20415737
	cellular response to UV-B	IDA		PMID:20415737
	zinc ion binding	IBA	PANTHER: PTN002918232 UniProtKB: P50238	PMID:21873635
	intrinsic apoptotic signaling pathway in response to DNA damage	IBA	PANTHER: PTN002918232 UniProtKB: P50238	PMID:21873635
	regulation of gene expression	IBA	PANTHER: PTN002918232 UniProtKB: P50238	PMID:21873635
FN1	angiogenesis	IEA	UniProtKB-KW:KW-0037	GO_REF:0000037
	regulation of protein phosphorylation	IDA		PMID:11792823
	protease binding	IPI	UniProtKB: P07711	PMID:22952693
	platelet degranulation	TAS		Reactome: R-HSA-114608
	signaling receptor binding	IPI	UniProtKB: P9WQP1	PMID:17849409
	integrin binding	IPI	UniProtKB: P05556	PMID:11792823
	extracellular matrix structural constituent	ISS	UniProtKB: F1SS24	GO_REF:0000024
	protein binding	IPI	UniProtKB: P9WIG5	PMID:10627046
	collagen binding	NAS		PMID:3024962
	extracellular region	NAS		PMID:14718574
	fibrinogen complex	IDA		PMID:3997886
	basement membrane	IEA	UniProtKB: P11276 ensembl: ENSMUSP00000054499	GO_REF:0000107
	extracellular space	IDA		PMID:15292204
	endoplasmic reticulum lumen	TAS		Reactome: R-HSA-8952289
	endoplasmic reticulum-Golgi intermediate compartment	IDA		PMID:15308636
	acute-phase response	IEA	UniProtKB-KW:KW-0011	GO_REF:0000037
	cell-substrate junction assembly	IEA	UniProtKB: P11276 ensembl: ENSMUSP00000054499	GO_REF:0000107
	cell adhesion	NAS		PMID:1423622

calcium-independent cell-matrix adhesion	IEA	JniProtKB: P11276 ensembl: ENSMUSP00000054499	GO_REF:0000107
protein C-terminus binding	IPI	JniProtKB: P9WK17	PMID:16677310
heparin binding	NAS		PMID:10075919
positive regulation of cell population proliferation	IDA		PMID:25834989
regulation of cell shape	IEA	JniProtKB-KW:KW-0133	GO_REF:0000037
response to wounding	NAS		PMID:7989369
positive regulation of gene expression	IDA		PMID:25834989
positive regulation of peptidase activity	IEA	GO:0016504	GO_REF:0000108
apical plasma membrane	IEA	JniProtKB: P11276 ensembl: ENSMUSP00000054499	GO_REF:0000107
peptidase activator activity	IEA	JniProtKB: P11276 ensembl: ENSMUSP00000054499	GO_REF:0000107
peptide cross-linking	IDA		PMID:3997886
cytokine-mediated signaling pathway	TAS		Reactome: R-HSA-6785807
enzyme binding	IPI	JniProtKB: Q9AIS0	PMID:12167537
extracellular matrix organization	TAS		Reactome: R-HSA-1474244
extracellular matrix	IDA		PMID:26571399
platelet alpha granule lumen	TAS		Reactome: R-HSA-481007
integrin activation	IMP		PMID:24658351
substrate adhesion-dependent cell spreading	IDA		PMID:16236823
endodermal cell differentiation	IDA		PMID:23154389
wound healing	IEA	JniProtKB: P11276 ensembl: ENSMUSP00000054499	GO_REF:0000107
identical protein binding	IPI	JniProtKB: P02751	PMID:17914904
proteoglycan binding	IDA		PMID:29030641
post-translational protein modification	TAS		Reactome: R-HSA-597592
cellular protein metabolic process	TAS		Reactome: R-HSA-392499
positive regulation of axon extension	IEA	JniProtKB: P11276 ensembl: ENSMUSP00000054499	GO_REF:0000107
positive regulation of fibroblast proliferation	IDA		PMID:25834989
leukocyte migration	TAS		Reactome: R-HSA-202733
chaperone binding	IPI	JniProtKB: P9WMJ9	PMID:17849409
interaction with symbiont	IDA		PMID:12167537
symbiotic process mediated by secreted substance	IDA		PMID:17849409
collagen-containing extracellular matrix	IDA		PMID:16157329
extracellular exosome	HDA		PMID:19056867
regulation of ERK1 and ERK2 cascade	IDA		PMID:11792823
blood microparticle	HDA		PMID:22516433
disordered domain specific binding	IPI	JniProtKB: O50835	PMID:15292204

	neural crest cell migration involved in autonomic nervous system development	IDA		PMID:26571399
	positive regulation of substrate-dependent cell migration, cell attachment to substrate	IDA		PMID:25834989
	negative regulation of transforming growth factor-beta secretion	IDA		PMID:25834989
	collagen-containing extracellular matrix	HDA		PMID:20551380
LYZ	retina homeostasis	HEP		PMID:23580065
	lysozyme activity	TAS		PMID:2829884
	extracellular region	TAS		Reactome: R-HSA-6798745
	extracellular space	HDA		PMID:16502470
	inflammatory response	TAS		PMID:366724
	antimicrobial humoral response	TAS		Reactome: R-HSA-6803157
	cytolysis	IEA	UniProtKB: KW:KW-0081	GO_REF:0000037
	killing of cells of other organism	IDA		PMID:9727055
	azurophil granule lumen	TAS		Reactome: R-HSA-6798751
	specific granule lumen	TAS		Reactome: R-HSA-6798749
	defense response to bacterium	IDA		PMID:21093056
	identical protein binding	IPI	UniProtKB: P61626	PMID:23353684
	neutrophil degranulation	TAS		Reactome: R-HSA-6798695
	cellular protein metabolic process	TAS		Reactome: R-HSA-392499
	defense response to Gram-positive bacterium	IDA		PMID:21093056
	extracellular exosome	HDA		PMID:19056867
	tertiary granule lumen	TAS		Reactome: R-HSA-6798745
	defense response to Gram-positive bacterium	IBA	MG: MGI:96897 MG: MGI:96902 PANTHER: PTN000892307 RGD:3026 UniProtKB: P61626	PMID:21873635
	defense response to Gram-negative bacterium	IBA	MG: MGI:96897 MG: MGI:96902 PANTHER: PTN000892307 RGD:3026	PMID:21873635
PYCARD	Golgi membrane	IDA		PMID:23229815
	myeloid dendritic cell activation	IMP		PMID:22732093
	protease binding	IPI	UniProtKB: P98073	PMID:24407287
	activation of innate immune response	IDA		PMID:21575908
	positive regulation of defense response to virus by host	IEA	UniProtKB: Q9EPB4 ensembl: ENSMUSP00000033056	GO_REF:0000107
	myeloid dendritic cell activation involved in immune response	ISS	UniProtKB: Q9EPB4	GO_REF:0000024

positive regulation of antigen processing and presentation of peptide antigen via MHC class II	ISS	UniProtKB: Q9EPB4	GO_REF:0000024
positive regulation of adaptive immune response	IMP		PMID:22732093
interleukin-6 receptor binding	IPI	UniProtKB: P40189	PMID:24407287
protein binding	IPI	UniProtKB: O15553	PMID:11498534
tropomyosin binding	IPI	UniProtKB: P67936	PMID:24407287
extracellular region	TAS		Reactome: R-HSA-6798748
nucleus	ISS	UniProtKB: Q9EPB4	GO_REF:0000024
nucleoplasm	IDA		GO_REF:0000052
nucleolus	IDA		GO_REF:0000052
cytoplasm	NAS		PMID:12019269
mitochondrion	IDA		PMID:14730312
endoplasmic reticulum	IEA	UniProtKB-SubCell:SL-0095	GO_REF:0000039
cytosol	IDA		GO_REF:0000052
activation of cysteine-type endopeptidase activity involved in apoptotic process	NAS		PMID:12019269
inflammatory response	IEA	UniProtKB: Q9EPB4 ensembl: ENSMUSP00000033056	GO_REF:0000107
signal transduction	NAS		PMID:12019269
IkappaB kinase complex	TAS		PMID:12656673
cysteine-type endopeptidase activator activity involved in apoptotic process	NAS		PMID:12019269
regulation of autophagy	IEA	UniProtKB: Q9EPB4 ensembl: ENSMUSP00000033056	GO_REF:0000107
regulation of tumor necrosis factor-mediated signaling pathway	IMP		PMID:14730312
myosin I binding	IPI	UniProtKB: O00159	PMID:24407287
enzyme binding	IPI	UniProtKB: P49916	PMID:24407287
positive regulation of actin filament polymerization	ISS	UniProtKB: Q9EPB4	GO_REF:0000024
regulation of protein stability	ISS	UniProtKB: Q9EPB4	GO_REF:0000024
negative regulation of NF-kappaB transcription factor activity	IMP		PMID:16585594
Pyrin domain binding	IPI	UniProtKB: Q96P20	PMID:15030775
interleukin-1 beta production	IEA	UniProtKB: Q9EPB4 ensembl: ENSMUSP00000033056	GO_REF:0000107
negative regulation of interferon-beta production	IMP		PMID:19158675
positive regulation of interferon-gamma production	ISS	UniProtKB: Q9EPB4	GO_REF:0000024

positive regulation of interleukin-1 beta production	IMP		PMID:22267217
positive regulation of interleukin-6 production	ISS	UniProtKB: Q9EPB4	GO_REF:0000024
positive regulation of tumor necrosis factor production	IMP		PMID:16982856
protein-containing complex	IDA		PMID:22267217
tumor necrosis factor-mediated signaling pathway	IDA		PMID:12656673
secretory granule lumen	TAS		Reactome: R-HSA-6798748
azurophil granule lumen	TAS		Reactome: R-HSA-6798751
positive regulation of activated T cell proliferation	ISS	UniProtKB: Q9EPB4	GO_REF:0000024
intrinsic apoptotic signaling pathway in response to DNA damage by p53 class mediator	IMP		PMID:14730312
identical protein binding	IPI	UniProtKB: Q9JULZ3	PMID:24630722
protein homodimerization activity	IDA		PMID:15030775
neuronal cell body	IEA	UniProtKB: G3V8L1 ensembl: ENSRNOP00000026699	GO_REF:0000107
positive regulation of apoptotic process	IDA		PMID:12646168
regulation of GTPase activity	IEA	UniProtKB: Q9EPB4 ensembl: ENSMUSP00000033056	GO_REF:0000107
negative regulation of I-kappaB kinase/NF-kappaB signaling	IDA		PMID:12486103
positive regulation of cysteine-type endopeptidase activity involved in apoptotic process	IDA		PMID:15030775
neutrophil degranulation	TAS		Reactome: R-HSA-6798695
ion channel binding	IEA	UniProtKB: G3V8L1 ensembl: ENSRNOP00000026699	GO_REF:0000107
macropinocytosis	ISS	UniProtKB: Q9EPB4	GO_REF:0000024
innate immune response	IEA	UniProtKB: KW:KW-0399	GO_REF:0000037
positive regulation of JNK cascade	IMP		PMID:21487011
protein dimerization activity	IDA		PMID:24531343
positive regulation of interleukin-1 beta secretion	IDA		PMID:15030775
positive regulation of phagocytosis	ISS	UniProtKB: Q9EPB4	GO_REF:0000024
defense response to Gram-negative bacterium	IMP		PMID:16982856
positive regulation of T cell activation	IMP		PMID:22732093
positive regulation of DNA-binding transcription factor activity	IDA		PMID:19494289

positive regulation of NF-kappaB transcription factor activity	IDA		PMID:12646168
protein homooligomerization	IDA		PMID:24531343
defense response to virus	IDA		PMID:21575908
positive regulation of ERK1 and ERK2 cascade	IMP		PMID:21487011
BMP receptor binding	IPI	UniProtKB: Q13873	PMID:24407287
cellular response to lipopolysaccharide	IDA		PMID:12486103
cellular response to interleukin-1	IDA		PMID:12486103
cellular response to tumor necrosis factor	IDA		PMID:12486103
negative regulation of protein serine/threonine kinase activity	IDA		PMID:12486103
intrinsic apoptotic signaling pathway by p53 class mediator	IMP		PMID:14730312
NLRP1 inflammasome complex	IDA		PMID:12191486
NLRP3 inflammasome complex	IDA		PMID:15030775
positive regulation of chemokine secretion	IMP		PMID:21487011
positive regulation of release of cytochrome c from mitochondria	IDA		PMID:14730312
AIM2 inflammasome complex	IDA		PMID:19158676
activation of cysteine-type endopeptidase activity	IEA	UniProtKB: Q9EPB4 ensembl: ENSMUSP00000033056	GO_REF:0000107
negative regulation of cytokine production involved in inflammatory response	IMP		PMID:24531343
positive regulation of T cell migration	ISS	UniProtKB: Q9EPB4	GO_REF:0000024
positive regulation of interleukin-8 secretion	IMP		PMID:16982856
positive regulation of interleukin-6 secretion	IMP		PMID:16982856
positive regulation of cysteine-type endopeptidase activity	IDA		PMID:19158676
positive regulation of interleukin-10 secretion	IMP		PMID:16982856
positive regulation of extrinsic apoptotic signaling pathway	IDA		PMID:16964285
regulation of intrinsic apoptotic signaling pathway	IDA		PMID:14730312
IkappaB kinase complex	IDA		PMID:12486103

	apoptotic process	IBA	FB:FBgn0010501 FB:FBgn0019972 FB:FBgn0020381 FB:FBgn0028381 FB:FBgn0033659 MGi:MGi:107739 MGi:MGi:109383 MGi:MGi:1261423 MGi:MGi:1277950 MGi:MGi:1312922 MGi:MGi:97295 PANTHER:PTN000047947 RGD:2274 RGD:2275 RGD:61867 RGD:620944 RGD:620945 RGD:69274 UniProtKB:O15519 UniProtKB:P42574 UniProtKB:P55210 UniProtKB:P55211 UniProtKB:Q14790 WB:WBGene00000417 ZFIN:ZDB-GENE-011210-1	PMID:21873635
	intrinsic apoptotic signaling pathway in response to DNA damage	IBA	PANTHER: PTN000048135 UniProtKB: Q9ULZ3	PMID:21873635
	cysteine-type endopeptidase activity involved in apoptotic process	IBA	FB: FBgn0010501 FB: FBgn0019972 MGi: MG:107739 MGi: MG:109383 MGi: MG:1261423 MGi: MG:97295 PANTHER: PTN000047947 UniProtKB: P42574 UniProtKB: P55210 UniProtKB: P55211 UniProtKB: P55212 UniProtKB: Q14790 UniProtKB: Q92851 WB: WBGene00000417	PMID:21873635
	extrinsic apoptotic signaling pathway in absence of ligand	IBA	MGi: MG:97295 PANTHER: PTN000048135	PMID:21873635
	cytoplasm	IBA	FB:FBgn0010501 FB:FBgn0019972 FB:FBgn0020381 FB:FBgn0028381 FB:FBgn0033051 MGi:MGi:107739 MGi:MGi:1261423 MGi:MGi:1277950 MGi:MGi:1312922 MGi:MGi:1336166 MGi:MGi:1931465 MGi:MGi:97295 PANTHER:PTN000047947 RGD:2274 RGD:2275 RGD:61867 RGD:620944 RGD:620945 RGD:621758 RGD:69274 RGD:70967 UniProtKB:F1NL59 UniProtKB:O15519 UniProtKB:P31944 UniProtKB:P42574 UniProtKB:P49662 UniProtKB:P55210 UniProtKB:P55211 UniProtKB:P55212 UniProtKB:Q14790 UniProtKB:Q6UXS9 UniProtKB:Q8MKI5 UniProtKB:Q95ND5 UniProtKB:Q9ULZ3 WB:WBGene00000417	PMID:21873635
SAP30	histone deacetylase complex	IDA		PMID:9651585
	negative regulation of transcription by RNA polymerase II	IEA	UniProtKB: O88574 ensembl: ENSMUSP00000034022	GO_REF:0000107
	DNA binding	IEA	UniProtKB-KW:KW-0238	GO_REF:0000037
	transcription corepressor activity	IDA		PMID:9651585
	protein binding	IPI	UniProtKB: P51610	PMID:12670868
	nucleoplasm	IDA		GO_REF:0000052
	regulation of transcription, DNA-templated	IDA		PMID:9651585
	histone deacetylation	IEA	GO:0004407	GO_REF:0000108
	skeletal muscle cell differentiation	IEA	UniProtKB: O88574 ensembl: ENSMUSP00000034022	GO_REF:0000107
	metal ion binding	IEA	UniProtKB-KW:KW-0479	GO_REF:0000037
	transcription coregulator activity	IBA	PANTHER: PTN000328752 UniProtKB: O75446	PMID:21873635
	regulation of transcription, DNA-templated	IBA	PANTHER: PTN000328752 UniProtKB: O75446	PMID:21873635
	histone deacetylase activity	IBA	PANTHER: PTN000328752 SGD: S000004876	PMID:21873635
	histone deacetylase complex	IBA	PANTHER: PTN000328752 UniProtKB: O75446 UniProtKB: Q9HAJ7	PMID:21873635
ESRRG	nuclear chromatin	ISA	tfclass:2.1.1	GO_REF:0000113
	RNA polymerase II regulatory region sequence-specific DNA binding	IEA	UniProtKB: P62509 ensembl: ENSMUSP00000027906	GO_REF:0000107

	DNA-binding transcription factor activity, RNA polymerase II-specific	ISA	class:2.1.1	GO_REF:0000113
	DNA-binding transcription activator activity, RNA polymerase II-specific	IEA	UniProtKB: P62509 ensembl: ENSMUSP00000027906	GO_REF:0000107
	steroid hormone receptor activity	IEA	InterPro: IPR001723 InterPro: IPR024178 InterPro: IPR027289	GO_REF:0000002
	nuclear receptor activity	IEA	InterPro: IPR003078	GO_REF:0000002
	steroid binding	IEA	InterPro: IPR024178 InterPro: IPR027289	GO_REF:0000002
	protein binding	IPI	UniProtKB: Q61026	PMID:10428842
	nucleoplasm	TAS		Reactome: R-HSA-376419
	regulation of transcription, DNA-templated	IDA		PMID:23836911
	transcription initiation from RNA polymerase II promoter	TAS		Reactome: R-HSA-383280
	zinc ion binding	IEA	InterPro: IPR001628 InterPro: IPR013088 InterPro: IPR024178	GO_REF:0000002
	steroid hormone mediated signaling pathway	IEA	GO:0003707	GO_REF:0000108
	positive regulation of transcription, DNA-templated	ISS	UniProtKB: P62509	GO_REF:0000024
	positive regulation of transcription by RNA polymerase II	IEA	UniProtKB: P62509 ensembl: ENSMUSP00000027906	GO_REF:0000107
	retinoic acid receptor signaling pathway	IEA	InterPro: IPR003078	GO_REF:0000002
	AF-2 domain binding	ISS	UniProtKB: P62509	GO_REF:0000024
ESRRG	positive regulation of cold-induced thermogenesis	ISS	UniProtKB: P62509	PMID:17229846

TAS, traceable author statement; IEA, Inferred from Electronic Annotation; IBA, Inferred from Biological aspect of Ancestor; IDA, Inferred from Direct Assay; IMP, Inferred from Mutant Phenotype; HDA, Inferred from High Throughput Direct Assay; IPI, Inferred from Physical Interaction; ISS, Inferred from Sequence or structural Similarity; NAS, Non-traceable Author Statement; IEP, Inferred from Expression Pattern; HEP, Inferred from High Throughput Expression Pattern; ISA, Inferred from Sequence Alignment.

Table S2 The Gene Ontology (GO) and Kyoto Encyclopedia of Genes and Genomes (KEGG) pathways analysis among co-expressed differentially genes of hypertension-related renal cell carcinoma and their predicted miRNAs

Genes	Predicted miRNAs	Category	Function	P value
BCAT1	hsa-let-7f-5p	KEGG pathway	ECM-receptor interaction	7.00E-17
	hsa-let-7g-5p		Amoebiasis	0.004634
	hsa-let-7i-5p		Signaling pathways regulating pluripotency of stem cells	0.006974
	hsa-miR-218-5p		PI3K-Akt signaling pathway	0.023169
	hsa-miR-98-5p		Wnt signaling pathway	0.026951
		GO terms	Fc-epsilon receptor signaling pathway	0.001352
			Cellular component assembly	0.001352
			Macromolecular complex assembly	0.001682
			Regulation of transcription from RNA polymerase II promoter in response to hypoxia	0.002075
			Neurotrophin TRK receptor signaling pathway	0.002075
			Protein complex assembly	0.007927
			Extracellular matrix disassembly	0.009607
			Small molecule metabolic process	0.00984
CORO1A	hsa-miR-301b-3p	KEGG pathway	Estrogen signaling pathway	0.00043
	hsa-miR-370-3p		Endocytosis	0.007175
	hsa-miR-454-3p		Gap junction	0.01461
	hsa-miR-504-5p	GO terms	Cellular protein modification process	6.38E-12
	hsa-miR-744-5p		Neurotrophin TRK receptor signaling pathway	2.70E-09
			Nervous system development	0.000246
			Membrane organization	0.000541
			Small molecule metabolic process	0.000541
CRIP1	hsa-miR-221-5p	KEGG pathway	ECM-receptor interaction	4.65E-11
	hsa-miR-4720-5p		Fatty acid elongation	0.001276
		GO terms	Cellular nitrogen compound metabolic process	0.002025
			Gene expression	0.004677

ESRRG	hsa-miR-137	KEGG pathway	Prion diseases	1.03E-12
	hsa-miR-148a-3p		ErbB signaling pathway	3.66E-06
	hsa-miR-152-3p		Adherens junction	0.000149
	hsa-miR-205-5p		Oxytocin signaling pathway	0.000746
	hsa-miR-7-5p		Proteoglycans in cancer	0.0008
		GO terms	Neurotrophin TRK receptor signaling pathway	1.55E-25
			Fc-epsilon receptor signaling pathway	4.15E-20
			Epidermal growth factor receptor signaling pathway	3.46E-18
			Cellular component assembly	5.38E-14
			Blood coagulation	1.10E-11
			Fibroblast growth factor receptor signaling pathway	8.45E-11
FN1	hsa-miR-144-3p	KEGG pathway	Hippo signaling pathway	3.15E-05
	hsa-miR-199a-3p		Thyroid hormone signaling pathway	0.000558
	hsa-miR-200b-3p		ErbB signaling pathway	0.000597
	hsa-miR-200c-3p		Gap junction	0.000597
	hsa-miR-429	GO terms	Cellular nitrogen compound metabolic process	4.19E-52
			Cellular protein modification process	2.64E-41
			Neurotrophin TRK receptor signaling pathway	1.67E-13
			Fc-epsilon receptor signaling pathway	5.93E-13
			Blood coagulation	6.73E-09
LYZ	hsa-miR-1-3p	KEGG pathway	Proteoglycans in cancer	0.000101
	hsa-miR-140-5p		Gap junction	0.001277
	hsa-miR-206		Rap1 signaling pathway	0.003687
	hsa-miR-23b-3p		Glutamatergic synapse	0.004599
	hsa-miR-452-5p		Renal cell carcinoma	0.00613
		GO terms	Neurotrophin TRK receptor signaling pathway	3.81E-15
			Transcription, DNA-templated	4.14E-15
			Fc-epsilon receptor signaling pathway	3.12E-13
			Epidermal growth factor receptor signaling pathway	2.15E-12
			Cellular component assembly	2.15E-12
			Macromolecular complex assembly	6.93E-10
PYCARD	hsa-miR-383-5p	KEGG pathway	Thyroid hormone synthesis	1.35E-14
			Fatty acid degradation	7.57E-07
			Adrenergic signaling in cardiomyocytes	0.00013

			Fatty acid metabolism	0.000343
			Ubiquinone and other terpenoid-quinone biosynthesis	0.004631
			Valine, leucine and isoleucine degradation	0.00753
		GO terms	Cellular nitrogen compound metabolic process	0.007499
SAP30	hsa-miR-30a-5p	KEGG pathway	Mucin type O-Glycan biosynthesis	1.84E-05
	hsa-miR-30b-5p		Axon guidance	0.001843
	hsa-miR-30c-5p		Gap junction	0.006902
	hsa-miR-30d-5p		Morphine addiction	0.006902
	hsa-miR-30e-5p		Arrhythmogenic right ventricular cardiomyopathy (ARVC)	0.006902
		GO terms	Fc-epsilon receptor signaling pathway	2.53E-11
			Neurotrophin TRK receptor signaling pathway	2.74E-07
			Post-translational protein modification	3.24E-06
			Epidermal growth factor receptor signaling pathway	5.30E-06
			Blood coagulation	1.42E-05
			Platelet activation	0.000704
			Cell death	0.005609